Kinetic Resolution Polymerization Enabled Chemical Synthesis of Perfectly Isotactic Polythioesters

Kun Li,[a] Jing-Liang Cheng,[b] Meng-Yuan Wang,[a] Wei Xiong,[a] Hao-Yi Huang,[a] Liang-Wen Feng,[b] Zhongzheng Cai,[a] & Jian-Bo Zhu[a]*

[a]National Engineering Laboratory of Eco-Friendly Polymeric Materials (Sichuan), College of Chemistry, Sichuan University, 29 Wangjiang Rd, Chengdu, 610064, P. R. China

[b]Key Laboratory of Green Chemistry and Technology of Ministry of Education, College of Chemistry, Sichuan University, Chengdu, 610064, P. R. China

ABSTRACT: Isotactic polythioesters (PTEs) that were thioester analogs to polyhydroxyalkanoates (PHAs) has attracted growing attention due to their distinct properties. However, the development of chemically synthetic methods to prepare isotactic PTEs has long been an intricate endeavor. Herein, we report the successful synthesis of a perfectly isotactic PTE via stereocontrolled ring-opening polymerization. This binaphthalene-salen alumnium (SalBinam-Al) catalyst promoted a robust polymerization of *rac*-α-substituted-β-propiothiolactones (*rac*-BTL and *rac*-PTL) with highly kinetic resolution and afforded perfectly isotactic P(BTL) and P(PTL) with M_n up to 276 kDa. More impressively, the isotactic P(BTL) contributed to forming a supramolecular stereocomplex with improved thermal property of T_m = 204 °C. Ultimately, this kinetic resolution polymerization enabled the facile isolation of enantiopure (*S*)-BTL, which could efficiently convert to an important pharmaceutical building block (*S*)-2-benzyl-3-mercapto-propanoic acid. Isotactic P(PTL) served as a tough and ductile material comparable to the commercialized polyolefins. This synthetic system allowed to access of isotactic PTEs, establishing a powerful platform for the discovery of sustainable plastics.

INTRODUCTION

The growing accumulation of plastic waste have become major threats to the planet.[1,2] The development of biodegradable polymers has been considered as an appealing and promising approach to addressing plastic pollution.[3–6] Polyhydroxyalkanoates (PHAs) that were naturally produced by bacteria and other microorganism have emerged as state-of-the-art bioplastic owing to their inherent biodegradability and excellent biocompatibility.[7–9] The large PHA family comprising diverse structures offered tunable material performance and a wide range of applicability. Importantly, the perfect isotacticity with each pendant group having exclusively (*R*)-configuration is the key to the superior thermal, mechanical, and biodegradable performance of PHAs.[10] The incorporation of sulfur element into polymers has been exploited to impart the resulting materials with unique properties such as outstanding optical and electrical features, potential coordinating ability to heavy metal ions, and chemical recyclability.[11–23] Consequently, this sulfur reformation to prepare the thioester analogs to PHAs by replacing the oxoester linkages with thioester counterparts are of great interest, which would deliver distinct material performance and pave the way to more diversified applications. However, these desired isotactic polythioesters (PTEs) are remained less explored due to their challenging preparation. Poly(3-mercaptovalerate) (P3TB) that was biosynthesized by engineered *Escherichia coli* is one of the very first reported isotactic PTE which exhibited different physical properties from poly(3-hydroxybutyrate) (P3HB).[24] However, the current biosynthetic method is still facing many formidable challenges including limited scalability and high production cost. Chemical synthetic route via ring-opening polymerization (ROP) of thiolactones (TLs) to prepare isotactic PTEs would serve as a desirable alternative to circumvent the abovementioned disadvantages.

The development of chemically synthetic methods to prepare isotactic polythioesters has long been an intricate endeavor (Figure 1). Direct ROP of enantiopure TLs is supposed to be a straightforward route, but the availability of enantiopure TLs is limited. Moreover, the occurrence of an undesirable and inevitable racemization appeared as another major obstacle to accomplish efficient stereoretentive polymerization of enantiopure TLs. Racemization is a common phenomenon found in thioester chemistry due to the increased

acidity of α-methine hydrogen.[25,26] In fact, this racemization phenomenon not only complicates the ROP of enantiopure TLs but also presents challenges for the stereoselective ROP of racemic thiolactones. Moreover, the poisoning of the organometallic catalysts by sulfide chain-end and the occurrence of undesirable chain-transfer side reactions pose additional obstacles to achieving highly stereoselective ROP of *rac*-TLs. Therefore, to control the stereoselectivity in the ROP of *rac*-TLs remains challenging. In contrast to numerous catalytic systems that were reported to facilitate the chemical synthesis of stereoregular PHAs through stereoselective ROP of racemic four-membered lactones,[27–38] only one elegant work from Capentier, Guillaume, and coworkers has manifested the feasibility of stereocontrolled ROP of racemic four-membered thiolactone to prepare isotactic cyclic P(3TB) with a P_m of 0.90 (P_m is the probability of *meso* linkages between monomer unites) at −80 °C.[39] This precedent prompted us to explore new catalysts and TLs to achieve the chemical synthesis of isotactic PTEs.

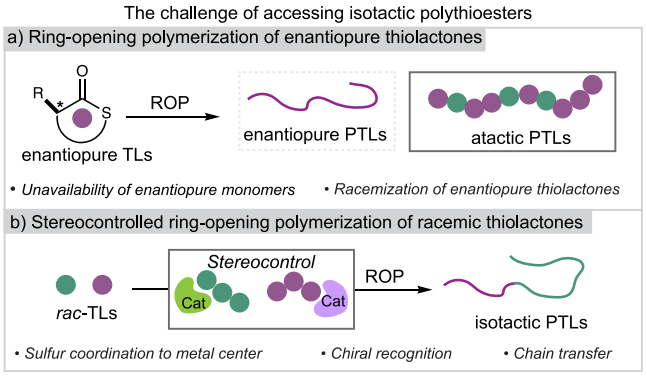

Figure 1. The Challenge of accessing isotactic polythioesters (PTLs). a) Ring-opening polymerization of enantiopure thiolactones. b) Stereocontrolled ring-opening polymerization of racemic thiolactiones.

We envisioned that a relatively high steric hindrance on the α-position of TL monomer could effectively inhibit the undesirable chain-transfer side reaction to achieve well-controlled polymerization fashion. As proof of concept, *rac*-α-benzyl-β-propiothiolactone (*rac*-BTL) was targeted since its derivative (*S*)-2-benzyl-3-mercapto-propanoic acid ((*S*)-BMPA) acted as a valuable building block for biomedince.[40,41] Excitingly, the synthesis of perfectly isotactic P(BTL) is accomplished by a highly kinetic resolution ROP of *rac*-BTL with an optimized racemic binaphthalene-salen aluminum catalyst. Mechanistic investigation revealed this catalytic system favored an enantiomorphic-site control mechanism with a kinetic resolution factor of 142. More impressively, these isotactic P(BTL) contributed to forming a stereocomplexed product with a significantly increased T_m of 204 °C. Ultimately, this kinetic resolution polymerization allowed for the facile isolation of (*S*)-BTL, which was capable to convert to (*S*)-BMPA efficiently. This kinetic resolution polymerization strategy was further applied for the preparation of isotactic P(PTL) bearing isopropyl side chains. The obtained isotactic P(PTL) demonstrated distinct thermal and mechanical performance, demonstrating a powerful platform towards isotactic PTEs with tunable properties.

RESULTS AND DISCUSSION

Stereoselective ring-opening polymerization. *Rac*-BTL was prepared on gram-scale with an overall yield of 49% according to a modified literature procedure (Scheme S1).[42] Initially, commercially available La[N(SiMe$_3$)$_2$]$_3$ (La) was examined for the ROP of *rac*-BTL in presence of benzyl mercaptan (BnSH) as an initiator at room temperature, which afforded atactic P(BTL) (P_m = 0.54). In the previous report, it's found that tetradentate alkoxy-amino-bis(phenolate) yttrium catalyst (Y),[43] β-diiminate zinc complex (Zn),[44] and aluminum-salen complexes (Al1, Al2, and Sal-BinamAl)[45–48] demonstrated powerful stereoselectivity towards the ROP of cyclic esters. Motivated by these seminal findings, the ROP of *rac*-BTL with these catalysts was next investigated at a [*rac*-BTL]:[Cat.]:[BnSH] ratio of 100:1:1 (Table 1 and Table S2). Catalyst Y facilitated the polymerization to completion within 1 min, producing P(BTL) with P_m of 0.35. The polymerization induced by Zn under a similar condition was sluggish and lack of stereoselectivity, approaching 96% monomer conversion in 10 h and yielding atactic P(BTL) (P_m = 0.48) (Table 1, entry 3). The cyclohexanediamine-based salen Al1 exhibited limited catalytic activity for the polymerization (Table 1, entry 4). Changing the chiral scaffold to binaphthalene-salen Al2 allowed for a boost for polymerization activity albeit low stereoselectivity (Table 1, entry 5).

In an effort to engineer this salen system with improving stereoselectivity, a steric modification of the substituent on the *ortho* position from hydrogen (H) to *tert*-butyl groups (*t*-Bu) was executed to prepare *rac*-SalBinam-Al. Gratifyingly, *rac*-SalBinam-Al promoted perfectly enantioselective polymerization of *rac*-BTL, creating perfectly isotactic P(BTL) with P_m > 0.99 (Table 1, entry 6). It should be noted that the resulting isotactic P(BTL) precipitated out from the homogenous toluene solution during the polymerization process due to its decreased solubility in comparison with atactic P(BTL). Instead, all the obtained P(BTL) samples was characteried by size exclusion chromatography (SEC) in 1,2,4-$C_6H_3Cl_3$ at 150 °C. Increasing the

Table 1. Ring-opening polymerization results of *rac*-BTL.[a]

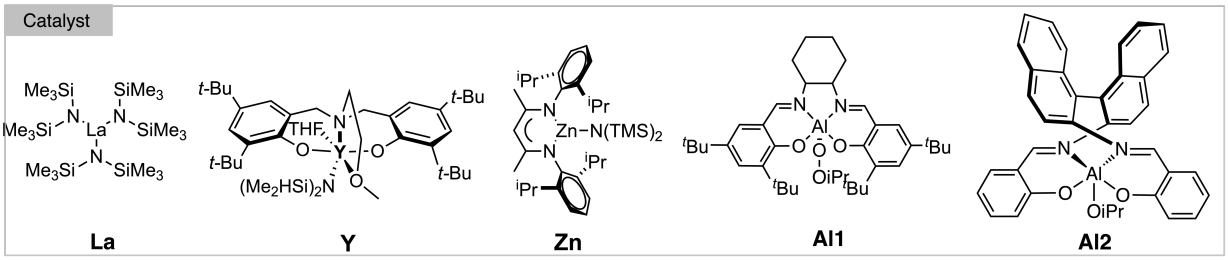

Run	Cat.	[M]:[Cat.]:[BnSH]	Time (min)	Conv. (%)[b]	M_n[c] (kDa)	$Đ$[c]	P_m[d]
1	**La**	100:1:1	5	>99	14.6[e]	4.12[e]	0.54
2	**Y**	100:1:1	1	>99	19.8[e]	1.32[e]	0.35
3	**Zn**	100:1:1	10 h	96	11.5[e]	1.39[e]	0.48
4	**Al1**	100:1:0	40	-	-	-	-
5	**Al2**	100:1:0	6	>99	120[e]	1.47[e]	0.57
6	*rac*-SalBinamAl	100:1:1	15	>99	11.6	2.82	0.99
7	*rac*-SalBinamAl	200:1:1	25	89	23.6	2.72	0.99
8	*rac*-SalBinamAl	400:1:1	30	80	46.6	2.98	0.99
9	*rac*-SalBinamAl	800:1:1	90	70	81.9	2.82	0.99
10	*rac*-SalBinamAl	100:1:0	10	>99	113	2.04	0.99
11	*rac*-SalBinamAl	200:1:0	20	98	153	2.53	0.99
12	*rac*-SalBinamAl	400:1:0	70	>99	232	2.40	0.99
13	*rac*-SalBinamAl	800:1:0	100	>99	243	2.43	0.99
14	(*R*)-SalBinamAl	100:1:1	18	53	6.7	2.24	0.99
			20 h	95	13.4	2.14	0.99
15	(*S*)-SalBinamAl	100:1:1	18	53	6.1	2.27	0.99
			20 h	94	11.9	2.24	0.99
16[f]	*rac*-SalBinamAl	800:1:0	8	92	170	2.69	0.99
17[f]	*rac*-SalBinamAl	1600:1:0	30	81	195	2.71	0.99
18[f]	*rac*-SalBinamAl	2000:1:0	35	89	224	2.61	0.99

[a]Conditions: The reactions were performed in a dry argon atmosphere, room temperature, monomer = 178 mg (1 mmol), [1 M], initiator = BnSH, solvent = toluene. [b]Determined by ^{1}H NMR spectroscopy. [c]Number-average molecular weight (M_n) and dispersity index ($Đ = M_w/M_n$) determined by size exclusion chromatography (SEC) in 1,2,4-$C_6H_3Cl_3$ at 150 °C versus polystyrene standards. [d]P_m is the probability of *meso* linkages between monomer units determined by ^{13}C NMR spectroscopy. [e]Number-average molecular weight (M_n) and dispersity index ($Đ = M_w/M_n$) determined by SEC in THF at 40 °C versus polystyrene standards. [f]The reaction temperature was 80 °C.

[*rac*-BTL]:[Cat.]:[BnSH] ratio from 100:1:1 to 800:1:1 led to an increase in polymer number-average molecular weight (M_n) from 11.6 to 81.9 kDa (Table 1, entries 6−9). The broad dispersity ($Đ$ = 2.72−2.98) and the inconsistency between the experimental M_n values and theoretical values could be attributed to the heterogenous polymerization process. Interestingly, the polymerization in absence of the initiator BnSH furnished unexpected high-M_n P(BTL) ranging from 113 to 243 kDa while preserving the perfect isoselectivity (Table 1, entries 10−13). We inferred the inefficient initiation process of SalBinam-Al led to this phenomenon.

To fully elucidate the stereoselective performance of SalBinam-Al, enantiopure (*R*)-SalBinam-Al and (*S*)-SalBinam-Al were prepared and evaluated for the polymerization (Figure 2a). The structure of (*R*)-SalBinam-Al was confirmed by single crystal X-ray diffraction analysis (Figure 2b). The ROP mediated by (*R*)-SalBinam-Al reached 53% monomer conversion in 18 min and furnished isotactic P[(*R*)-BTL)] with a M_n of 6.7 kDa (P_m > 0.99) (Table 1, entry 14). The remained unreacted monomers (*S*)-BTL were determined in 99% ee (enantiomeric excess) according to the chiral high-performance liquid chromatography (HPLC) analysis (Figure S97), indicative of an enantiomorphic-site control mechanism. Continuingly, it further required 20 h to achieve 95% monomer conversions and afford isoblock P(BTL) with a 2-fold increased M_n of 13.4 kDa. (*S*)-SalBinam-Al followed a similar reactivity and stereoselectivity patterns of its enantiomer (*R*)-SalBinam-Al, delivering isotactic P[(*S*)-BTL)] (P_m >

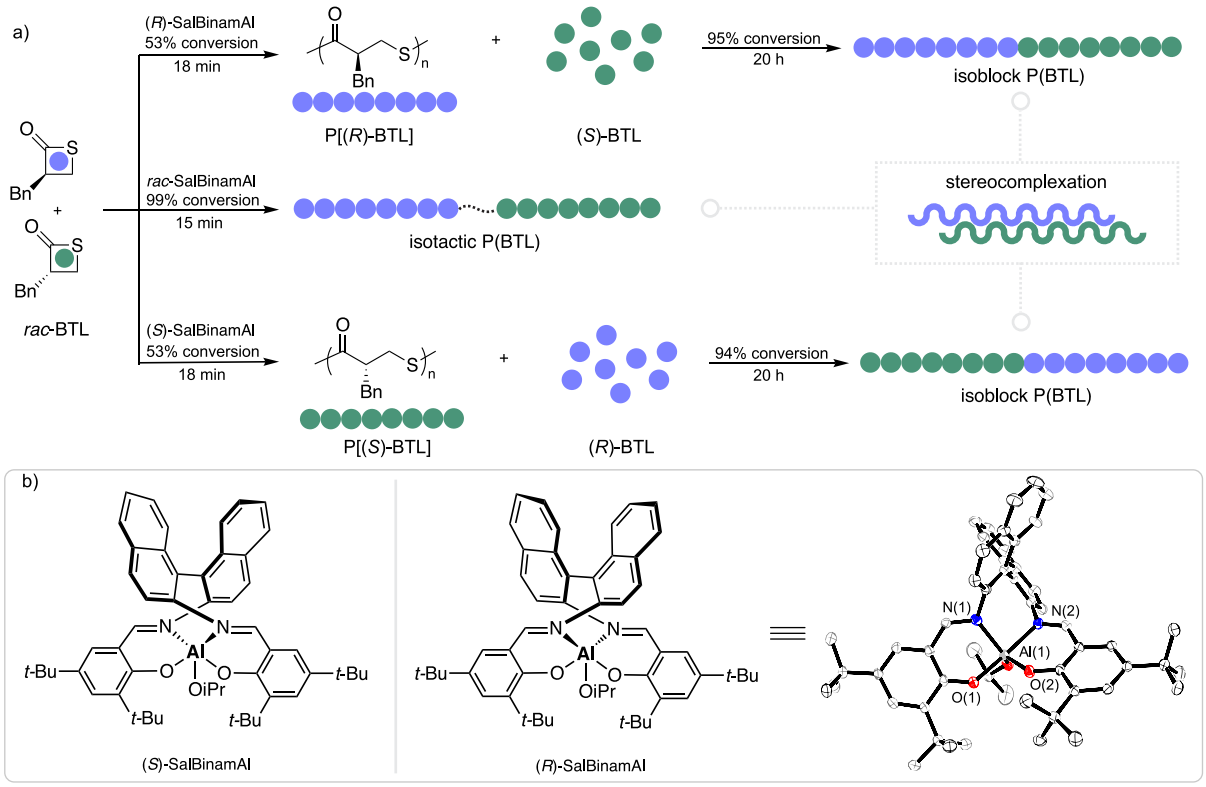

Figure 2. Stereocontrolled ring-opening polymerization of *rac*-BTL. a) Scheme of the stereocontrolled ROP of *rac*-BTL. b) Chemical structure of SalBinamAl and the X-ray crystal structure of (*R*)-SalBinamAl (ORTEP view, displacement ellipsoids drawn at 50% probability level). Hydrogen atoms have been omitted for clarity.

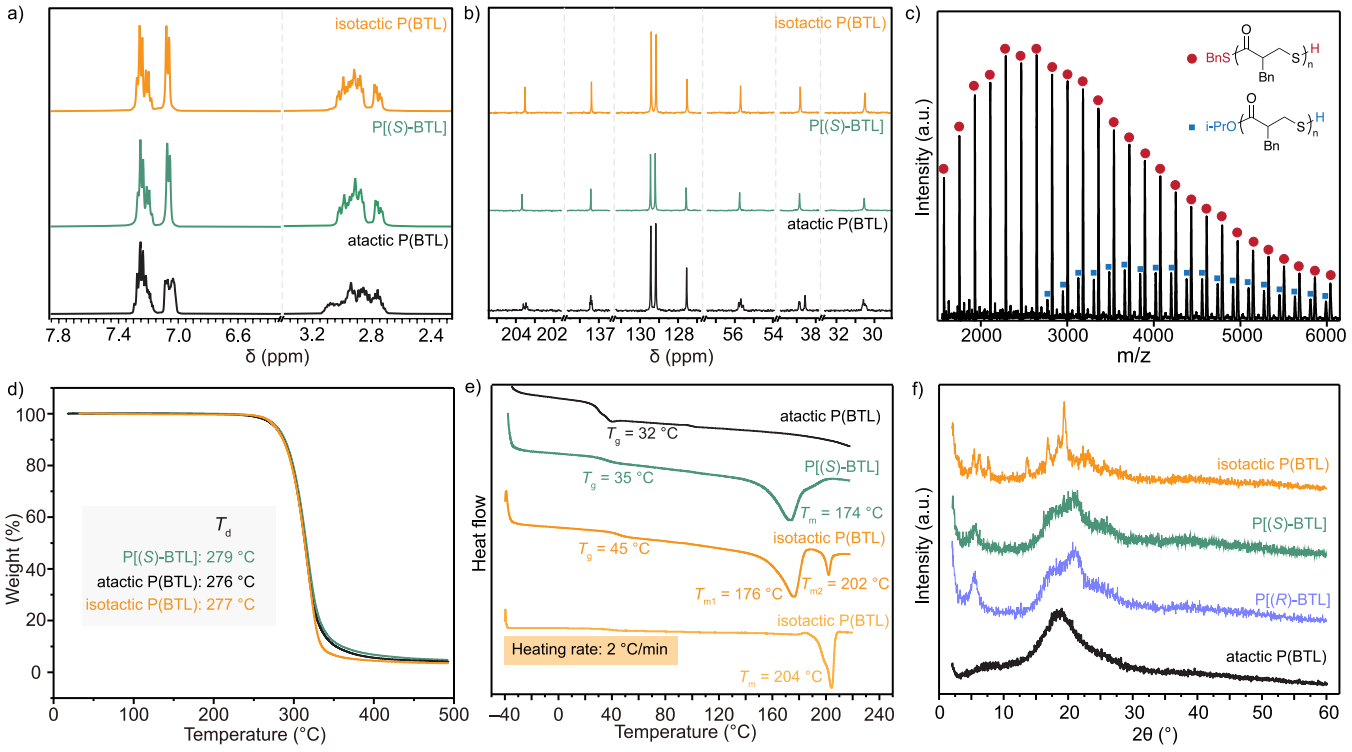

Figure 3. Characterization of P(BTL). a) ^{1}H NMR spectra of isotactic P(BTL), P[(*S*)-BTL], and atactic P(BTL). b) ^{13}C NMR spectra of isotactic P(BTL), P[(*S*)-BTL], and atactic P(BTL). c) MALDI-TOF mass spectrum of isotactic P(BTL). d) TGA curves of isotactic P(BTL), P[(*S*)-BTL], and atactic P(BTL). e) DSC curves of isotactic P(BTL), P[(*S*)-BTL], and atactic P(BTL). f) PXRD patterns of isotactic P(BTL), P[(*S*)-BTL], P[(*R*)-BTL], and atactic P(BTL).

0.99) in 53% conversion within 18 min and isoblock P(BTL) in 95% conversion at 20 h (Table 1, entry 15). These findings supported a kinetic resolution mechanism for the SalBinam-Al-mediated polymerization.

Characterization of P(BTL). To study the tacticity of P(BTL), isotacic P[(*S*)-BTL] was prepared as a reference via the ROP of (*S*)-BTL (Table S2, entry 5). (*S*)-3-(Acetylthio)-2-benzylpropanoic acid resolved by conventional crystallization separation of a pair of diastereomers of quinine salt was utilized as the starting material to synthesize enantiopure (*S*)-BTL (99% ee, Scheme S2). ^{1}H NMR and ^{13}C NMR spectroscopy were employzed to illustrate the stereoregularity of P(BTL). Despite the limited solubility in chloroform-d, these isotactic P(BTL) samples were able to be completely solubilized by the addition of HFIP (hexafluroisopropanol). Compared with the ^{1}H NMR spectrum of atactic P(BTL) having multiple broad chemical resonances at 3.2−2.6 ppm and 7.3−2.6 ppm, those of isotacic P(BTL) showcased clearly better resolved peaks (Figure 3a). Additionally, atactic P(BTL) displayed a complicated ^{13}C NMR spectrum with the appearance of multiple sets of resonance peaks at the full range (Figure 3b). In contrast, isotactic P(BTL) and P[(*S*)-BTL] illustrated the identical ^{13}C NMR spectra with single set of peaks associated to each carbon resonance, indicative of the perfect isotacticity.

Matrix-assisted laser desorption/ionization time-of-flight (MALDI-TOF) mass spectroscopy was conducted on a low-molecular-weight sample produced by [*rac*-BTL]:[*rac*-SalBinam-Al]:[BnSH] = 25:1:1 to disclose the microstructure of the obtained isotactic P(BTL). Its MALDI-TOF mass spectrum consisted of two series of molecular ion peaks with the spacing between the two neighboring molecular ion peaks consistent to the exact molar mass of the repeat unit (m/z = 178.05) (Figure 3c). Upon a linear fitting of the data (Figure S56), the major set of peaks corresponded to linear chains end-capped with BnSH groups, while the other series corresponded to linear chains with iPrOH as the chain ends due to the direct initiation by SalBinam-Al.

To probe the tacticity effect on the thermal performance of P(BTL), thermal gravimetric analysis (TGA) and differential scanning calorimetry (DSC) experiments were carried out. All these P(BTL) samples demonstrated similar thermal stability with T_d (onset decomposition temperature, defined by the temperature of 5% weight loss) of ~277 °C (Figure 3d), which was comparable to commercialized PHAs.[49,50] The DSC study revealed that atactic P(BTL) was amorphous materials with a glass transition temperature (T_g) of 32 °C. In a sharp contrast, isotacic P[(*S*)-BTL] exhibited a T_g of 35 °C and a melting transition temperature (T_m) of 174 °C, manifesting the significance of polymer stereoregularity (Figure 3e). Interestingly, the appearance of a new melting transition was observed at ~202 °C for isotactic P(BTL), which might ascribe to stereocomplexation between P[(*S*)-BTL] and P[(*R*)-BTL] blocks in the polymer material. The formation of stereocomplexation during the polymerization process might not be efficient due to the poor solubility of isotactic P(BTL), leading to the coexistence of two melting transitions. To address this issue, thermal processing at a slow heating rate of 2 °C/min was performed on this isotactic P(BTL) sample. The successful transformation to a clear T_m of 204 °C on the third heating scan suggested a fully stereocomplexed isotactic P(BTL). The PXRD patterns of this isotactic P(BTL) sample demonstrated more sharp and intense peaks in comparison with those of P[(*S*)-BTL] and P[(*R*)-BTL], providing corroborative evidence for its stereocomplexation effect (Figure 3f). The presence of stereocomplexation in this polymer system offered intriguing opportunity for the modulation of the material performance of P(BTL).

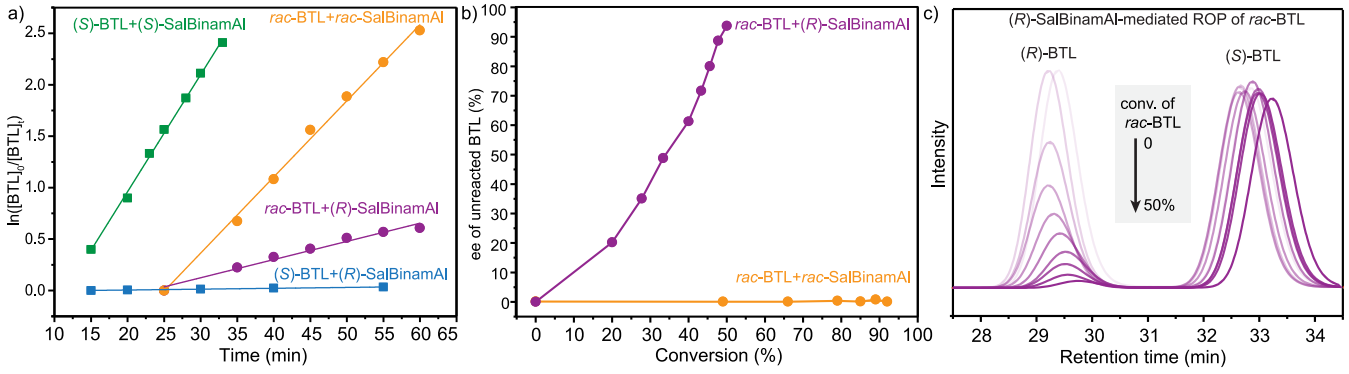

Figure 4. Mechanistic study of SalBinamAl-mediated kinetic resolution polymerization of *rac*-BTL. a) Kinetic plots of the ROP of BTL. 0.5 M in toluene, room temperature (rt), [BTL]:[SalBinamAl] = 400:1. b) ee (enantiomeric excess percentage) of unreacted BTL over conversion plots. c) Chiral HPLC spectra for the reaction solution of the (*R*)-SalBinam-mediated ROP of *rac*-BTL over monomer conversion.

Mechanistic study of SalBinamAl-mediated polymerization of *rac*-BTL. To gain further insights into the stereoselective mechanism of SalBinam-Al, kinetic study for the ROP of BTL with a [BTL]:[SalBinam-Al] ratio of 400:1 in 0.5 M toluene solution was performed via monitoring the change of monomer conversions over reaction time. The kinetic plots were summarized in Figure 4a. Interestingly, an induction period of 15−25 min was observed at the early stage for each plot and linear correlation between $\ln([BTL]_0/[BTL]_t)$ and reaction time was achieved if omitted their induction period. We speculated that the slow initiation of the isopropoxide ligand (OiPr) due to the high oxophilicity of the salen-based aluminum site was responsible for this induction period. This result also provided reasonable explanation for the unexpected high-Mn P(BTL) because of the low initiation efficiency. It should be noted that the addition of BnSH could not eliminate this induction period, indicating that BnSH worked as a chain transfer agent instead of an initiator during the polymerization process. This deduction was also confirmed by the absence of ^{1}H NMR spectral change of mixing SalBinam-Al and BnSH in 1:1 ratio (Figure S113). Attempts to accelerate the initiation step by increasing the polymerization temperature to 80 °C was next carried out, which expedited the polymerization process significantly (Table 1, entries 16−18). More impressively, the perfect isoselectivity of SalBinam-Al for the ROP of BTL was preserved at this industrially relevant temperature (80 °C), highlighting the superiority of our kinetic resolution polymerization strategy.

The polymerization of (*S*)-BTL catalyzed by (*S*)-SalBinam-Al showed a first-order kinetic with a slope ($k_{S/(S)\text{-BTL}}$) of 0.114 min^{-1}. In striking contrast, only trace conversion was detected for the polymerization of (*S*)-BTL by (*R*)-SalBinam-Al evidenced by a slope ($k_{R/(S)\text{-BTL}}$) of 0.0008 min^{-1}, illustrating that (*S*)-SalBinam-Al had an enantioselectivity for (*S*)-BTL. Collectively, these present data supported a kinetic resolution mechanism with very high $k_{S/(S)\text{-BTL}}/k_{R/(S)\text{-BTL}}$ ratio of 142 (Figure S111). Additionally, the rate constant for *rac*-SalBinam-Al-mediated ROP of *rac*-BTL ($k_{rac/rac\text{-BTL}}$) was calculated to be 0.074 min^{-1}. Chiral HPLC analysis of the unreacted monomer solution during this polymerization process revealed the ee remained close to 0 (Figure 4b), indicating the consumption of (*S*)-BTL and (*R*)-BTL at same time. As a comparison, (*R*)-SalBinam-Al accommodated the ROP of *rac*-BTL with a $k_{R/rac\text{-BTL}}$ of 0.019 min^{-1} accompanied by an increase in ee of the remained unreacted monomer solution. Only the consumption of (*R*)-BTL was detected until monomer conversion up to 50% by chiral HPLC analysis (Figure 4c). This result clearly identified the chiral preference of (*R*)-SalBinam-Al to (*R*)-BTL over (*S*)-BTL. Consequently, this enantiopure SalBinam-Al by creating a sterically chiral microenvironment enabled precise enantio-discrimination of BTL monomer, demonstrating an effective kinetic resolution polymerization mechanism.

The Application of kinetic resolution polymerization to prepare (*S*)-BMPA. Driven by the kinetic resolution polymerization, a facile isolation of (*S*)-BTL was accomplished by the (*R*)-SalBinam-mediated ROP of *rac*-BTL terminated at 54% monomer conversion. Notably, (*S*)-BTL was capable of converting to (*S*)-2-benzyl-3-mercapto-propanoic acid ((*S*)-BMPA, >99% ee) by a 2-step treatment (Figure 5). (*S*)-BMPA was found to be an effective inhibitor of carboxypeptidase A (CPA) and an important pharmaceutical building block for painkiller prodrugs such as RB-120.[40,41,51] (*S*)-BTL was able to undergo alcoholysis quantitatively by immersed in methanol solution of sulfuric acid. (*S*)-BMPA was collected in 79% yield upon the hydrolysis of the methyl ester intermediate with aqueous NaOH solution and acidification to pH = 1 (Figure S114). It represented an advanced approach for the preparation of (*S*)-BMPA in comparison with the sophisticated traditional patent separation method[52] (Scheme S2), which required multiple recrystallizations to yield (*S*)-BMPA. Overall, this ideal kinetic resolution polymerization not only offered an appealing strategy for the preparation of perfectly isotactic polythioesters but also established a direct pathway for the synthesis of enantiopure α-substituted four-membered thiolactones and enantiopure α-substituted 3-mercaptopropanoic acids.

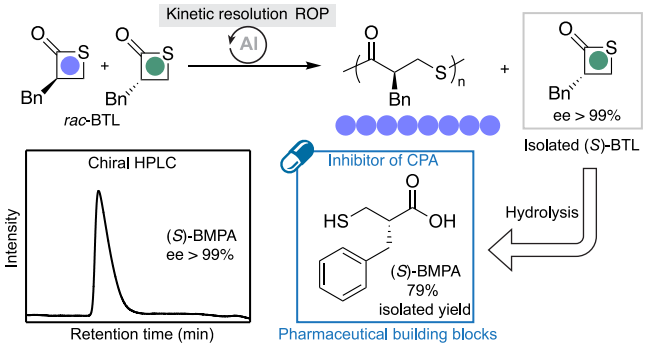

Figure 5. The application of SalBinamAl-mediated kinetic resolution polymerization to prepare (*S*)-BMPA.

Exploration of isotactic P(PTL). To further expand the application of our synthetic strategy, the ROP of *rac*-α-isopropyl-β-propiothiolactone (*rac*-PTL) was explored under a similar condition. Notably, this polymerization featured the well-established

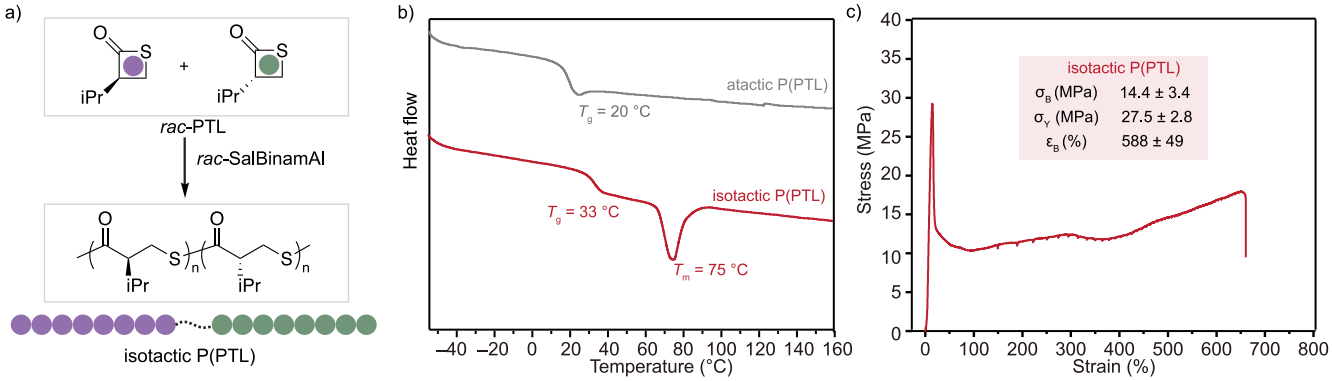

Figure 6. Synthesis and characterization of isotactic P(PTL). a) Stereocontrolled ring-opening polymerization of *rac*-PTL. b) DSC curves of isotactic P(PTL) and atactic P(PTL). c) Strain-stress curves of isotactic P(PTL).

isoselective fashion and yielded isotactic P(PTL) (P_m > 0.99) with a range of M_n values from 22.4 to 276 kDa and narrow $Đ$ (< 1.6) (Figure 6a, Table S10). It was noteworthy that the obtained isotactic P(PTL) exhibited improved solubility in comparison with P(BTL). In contrast to amorphous atactic P(PTL) having a T_g of 20 °C (Figure S126), DSC analysis disclosed that isotactic P(PTL) was semicrystalline with a T_m of 75 °C on the first heating scan (Figure 6b, Figure S127). The crystallinity and excellent processability of isotactic P(PTL) encouraged us to further investigate its mechanical property. Dog-bone shaped specimens were prepared by melt pressing at 100 °C and subjected to tensile testing experiments. The strain-stress curves revealed that P(PTL) represented a tough and ductile material with a yielding tensile strength (σ_Y) of 27.5 ± 2.8 MPa, a tensile strength at break (σ_B) of 14.4 ± 3.4 MPa, an ultimate elongation at break (ε_B) of 588 ± 49% and elastic modulus (E) of 321 ± 45 MPa (Figure 6c), which was comparable to the commercialized polyolefins.[53]

CONCLUSIONS

In summary, we have developed an efficient strategy to prepare isotactic PTEs via stereoselective ROP. This SalBinam-Al catalyst facilitated an effective and robust polymerization of *rac*-α-substituted-β-propiothiolactone (*rac*-BTL and *rac*-PTL) with highly kinetic resolution and allowed to access of perfectly isotactic PTEs with M_n up to 276 kDa. Mechanistic investigation of the ROP of *rac*-BTL illustrated an enantiomorphic-site control mechanism with a kinetic resolution factor of 142. Notably, this kinetic resolution polymerization was exploited for the facile preparation of the enantiopure (*S*)-BMPA, an important pharmaceutical building block. The obtained isotactic polythioester P(BTL) behaved as semicrystalline thermoplastic with a high melting temperature (~175 °C) and an enhancement of melting temperature to 204 °C was accomplished via stereocomplexation. Additionally, isotactic P(PTL) displayed tough and ductile mechanical performance with σ_B of 14.4 ± 3.4 MPa and ε_B of 588 ± 49%. Overall, we expected that this powerful synthetic platform will open up intriguing opportunities to access of isotactic PTEs with a wide range of notable properties and potential applications.

ASSOCIATED CONTENT

The Supporting Information is available free of charge on the ACS Publications website.
Experimental section, Analytical data, IR spectra, NMR spectral data and polymerization data. (PDF)

AUTHOR INFORMATION

Corresponding Author

*jbzhu@scu.edu.cn

Present Addresses

†If an author's address is different than the one given in the affiliation line, this information may be included here.

Author Contributions

All authors have given approval to the final version of the manuscript.

Notes

Any additional relevant notes should be placed here.

ACKNOWLEDGMENT

This work was supported by the National Key R&D Program of China (2021YFA1501700), the National Natural Science Foundation of China (22071163 and 22371194), and the Fundamental Research Funds from Sichuan University (2023SCUNL103). We thank Dr. Dongyan Deng from the College of Chemistry, Sichuan University, for NMR testing.

REFERENCES

(1) Stubbins, A.; Law, K. L.; Muñoz, S. E.; Bianchi, T. S.; Zhu, L. Plastics in the Earth System. *Science* **2021**, *373* (6550), 51–55. https://doi.org/10.1126/science.abb0354.

(2) MacLeod, M.; Arp, H. P. H.; Tekman, M. B.; Jahnke, A. The Global Threat from Plastic Pollution. *Science* **2021**, *373* (6550), 61–65. https://doi.org/10.1126/science.abg5433.

(3) Law, K. L.; Narayan, R. Reducing Environmental Plastic Pollution by

Designing Polymer Materials for Managed End-of-Life. *Nat. Rev. Mater.* **2022**, *7* (2), 104–116. https://doi.org/10.1038/s41578-021-00382-0.
(4) Zhu, Y.; Romain, C.; Williams, C. K. Sustainable Polymers from Renewable Resources. *Nature* **2016**, *540* (7633), 354–362. https://doi.org/10.1038/nature21001.
(5) Mohanty, A. K.; Wu, F.; Mincheva, R.; Hakkarainen, M.; Raquez, J.-M.; Mielewski, D. F.; Narayan, R.; Netravali, A. N.; Misra, M. Sustainable Polymers. *Nat. Rev. Methods Prim.* **2022**, *2* (1), 46. https://doi.org/10.1038/s43586-022-00124-8.
(6) Rosenboom, J.-G.; Langer, R.; Traverso, G. Bioplastics for a Circular Economy. *Nat. Rev. Mater.* **2022**, *7* (2), 117–137. https://doi.org/10.1038/s41578-021-00407-8.
(7) Sudesh, K.; Abe, H.; Doi, Y. Synthesis, Structure and Properties of Polyhydroxyalkanoates: Biological Polyesters. *Prog. Polym. Sci.* **2000**, *25* (10), 1503–1555. https://doi.org/https://doi.org/10.1016/S0079-6700(00)00035-6.
(8) Choi, S. Y.; Cho, I. J.; Lee, Y.; Kim, Y.-J.; Kim, K.-J.; Lee, S. Y. Microbial Polyhydroxyalkanoates and Nonnatural Polyesters. *Adv. Mater.* **2020**, *32* (35), 1907138. https://doi.org/https://doi.org/10.1002/adma.201907138.
(9) Dhaini, A.; Hardouin-Duparc, V.; Alaaeddine, A.; Carpentier, J.-F.; Guillaume, S. M. Recent Advances in Polyhydroxyalkanoates Degradation and Chemical Recycling. *Prog. Polym. Sci.* **2024**, *149*, 101781. https://doi.org/https://doi.org/10.1016/j.progpolymsci.2023.101781.
(10) Abe, H.; Matsubara, I.; Doi, Y.; Hori, Y.; Yamaguchi, A. Physical Properties and Enzymic Degradability of Poly(3-Hydroxybutyrate) Stereoisomers with Different Stereoregularities. *Macromolecules* **1994**, *27* (21), 6018–6025. https://doi.org/10.1021/ma00099a013.
(11) Mutlu, H.; Ceper, E. B.; Li, X.; Yang, J.; Dong, W.; Ozmen, M. M.; Theato, P. Sulfur Chemistry in Polymer and Materials Science. *Macromol. Rapid Commun.* **2019**, *40* (1), 1–51. https://doi.org/10.1002/marc.201800650.
(12) Xiong, W.; Lu, H. Recyclable Polythioesters and Polydisulfides with Near-Equilibrium Thermodynamics and Dynamic Covalent Bonds. *Sci. China Chem.* **2023**, *66* (3), 725–738. https://doi.org/10.1007/s11426-022-1418-9.
(13) Dai, J.; Xiong, W.; Du, M.-R.; Wu, G.; Cai, Z.; Zhu, J.-B. A Facile Approach towards High-Performance Poly(Thioether-Thioester)s with Full Recyclability. *Sci. China Chem.* **2023**, *66*, 251–258. https://doi.org/10.1007/s11426-022-1392-8.
(14) Cao, W.; Dai, F.; Hu, R.; Tang, B. Z. Economic Sulfur Conversion to Functional Polythioamides through Catalyst-Free Multicomponent Polymerizations of Sulfur, Acids, and Amines. *J. Am. Chem. Soc.* **2020**, *142* (2), 978–986. https://doi.org/10.1021/jacs.9b11066.
(15) Luo, M.; Zhang, X.-H.; Darensbourg, D. J. Poly(Monothiocarbonate)s from the Alternating and Regioselective Copolymerization of Carbonyl Sulfide with Epoxides. *Acc. Chem. Res.* **2016**, *49* (10), 2209–2219. https://doi.org/10.1021/acs.accounts.6b00345.
(16) Yue, T.-J.; Wang, L.-Y.; Ren, W.-M. The Synthesis of Degradable Sulfur-Containing Polymers: Precise Control of Structure and Stereochemistry. *Polym. Chem.* **2021**, *12*, 6650–6666. https://doi.org/10.1039/d1py01065d.
(17) Purohit, V. B.; Pięta, M.; Pietrasik, J.; Plummer, C. M. Recent Advances in the Ring-Opening Polymerization of Sulfur-Containing Monomers. *Polym. Chem.* **2022**, *13* (34), 4858–4878. https://doi.org/10.1039/D2PY00831A.
(18) Yue, T.-J.; Ren, W.-M.; Lu, X.-B. Copolymerization Involving Sulfur-Containing Monomers. *Chem. Rev.* **2023**, *123* (24), 14038–14083. https://doi.org/10.1021/acs.chemrev.3c00437.
(19) Wang, Y.; Zhu, Y.; Lv, W.; Wang, X.; Tao, Y. Tough While Recyclable Plastics Enabled by Monothiodilactone Monomers. *J. Am. Chem. Soc.* **2023**, *145* (3), 1877–1885. https://doi.org/10.1021/jacs.2c11502.
(20) Yuan, P.; Sun, Y.; Xu, X.; Luo, Y.; Hong, M. Towards High-Performance Sustainable Polymers via Isomerization-Driven Irreversible Ring-Opening Polymerization of Five-Membered Thionolactones. *Nat. Chem.* **2022**, *14* (3), 294–303. https://doi.org/10.1038/s41557-021-00817-9.
(21) Xiong, W.; Chang, W.; Shi, D.; Yang, L.; Tian, Z.; Wang, H.; Zhang, Z.; Zhou, X.; Chen, E.-Q.; Lu, H. Geminal Dimethyl Substitution Enables Controlled Polymerization of Penicillamine-Derived β-Thiolactones and Reversed Depolymerization. *Chem* **2020**, *6* (7), 1831–1843. https://doi.org/10.1016/j.chempr.2020.06.003.
(22) Shi, C.; McGraw, M. L.; Li, Z. C.; Cavallo, L.; Falivene, L.; Chen, E. Y. X. High-Performance Pan-Tactic Polythioesters with Intrinsic Crystallinity and Chemical Recyclability. *Sci. Adv.* **2020**, *6* (34), 1–12. https://doi.org/10.1126/sciadv.abc0495.
(23) Li, H.; Guillaume, S. M.; Carpentier, J.-F. Polythioesters Prepared by Ring-Opening Polymerization of Cyclic Thioesters and Related Monomers. *Chem. – An Asian J.* **2022**, *17* (17), e202200641. https://doi.org/https://doi.org/10.1002/asia.202200641.
(24) Lütke-Eversloh, T.; Fischer, A.; Remminghorst, U.; Kawada, J.; Marchessault, R. H.; Bögershausen, A.; Kalwei, M.; Eckert, H.; Reichelt, R.; Liu, S.-J.; Steinbüchel, A. Biosynthesis of Novel Thermoplastic Polythioesters by Engineered Escherichia Coli. *Nat. Mater.* **2002**, *1* (4), 236–240. https://doi.org/10.1038/nmat773.
(25) Li, M.; Tao, Y.; Tang, J.; Wang, Y.; Zhang, X.; Tao, Y.; Wang, X. Synergetic Organocatalysis for Eliminating Epimerization in Ring-Opening Polymerizations Enables Synthesis of Stereoregular Isotactic Polyester. *J. Am. Chem. Soc.* **2019**, *141* (1), 281–289. https://doi.org/10.1021/jacs.8b09739.
(26) Zhu, Y.; Li, M.; Wang, Y.; Wang, X.; Tao, Y. Performance-Advantaged Stereoregular Recyclable Plastics Enabled by Aluminum-Catalytic Ring-Opening Polymerization of Dithiolactone. *Angew. Chem. Int. Ed.* **2023**, *62* (24), e202302898. https://doi.org/https://doi.org/10.1002/anie.202302898.
(27) Thomas, C. M. Stereocontrolled Ring-Opening Polymerization of Cyclic Esters: Synthesis of New Polyester Microstructures. *Chem. Soc. Rev.* **2010**, *39* (1), 165–173. https://doi.org/10.1039/B810065A.
(28) Xie, X.; Huo, Z.; Jang, E.; Tong, R. Recent Advances in Enantioselective Ring-Opening Polymerization and Copolymerization. *Commun. Chem.* **2023**, *6* (1), 202. https://doi.org/10.1038/s42004-023-01007-z.
(29) Liao, X.; Su, Y.; Tang, X. Stereoselective Synthesis of Biodegradable Polymers by Salen-Type Metal Catalysts. *Sci. China Chem.* **2022**, *65* (11), 2096–2121. https://doi.org/10.1007/s11426-022-1377-5.
(30) Westlie, A. H.; Quinn, E. C.; Parker, C. R.; Chen, E. Y.-X. Synthetic Biodegradable Polyhydroxyalkanoates (PHAs): Recent Advances and Future Challenges. *Prog. Polym. Sci.* **2022**, *134*, 101608. https://doi.org/https://doi.org/10.1016/j.progpolymsci.2022.101608.
(31) Huang, H.-Y.; Xiong, W.; Huang, Y.-T.; Li, K.; Cai, Z.; Zhu, J.-B. Spiro-Salen Catalysts Enable the Chemical Synthesis of Stereoregular Polyhydroxyalkanoates. *Nat. Catal.* **2023**, *6* (8), 720–728. https://doi.org/10.1038/s41929-023-01001-7.
(32) Ligny, R.; Hänninen, M. M.; Guillaume, S. M.; Carpentier, J. F. Highly Syndiotactic or Isotactic Polyhydroxyalkanoates by Ligand-Controlled Yttrium-Catalyzed Stereoselective Ring-Opening Polymerization of Functional Racemic β-Lactones. *Angew. Chem. Int. Ed.* **2017**, *56* (35), 10388–10393. https://doi.org/10.1002/anie.201704283.
(33) Amgoune, A.; Thomas, C. M.; Ilinca, S.; Roisnel, T.; Carpentier, J. F. Highly Active, Productive, and Syndiospecific Yttrium Initiators for the Polymerization of Racemic β-Butyrolactone. *Angew. Chem. Int. Ed.* **2006**, *45* (17), 2782–2784. https://doi.org/10.1002/anie.200600058.
(34) Zhou, Z.; LaPointe, A. M.; Shaffer, T. D.; Coates, G. W. Nature-Inspired Methylated Polyhydroxybutyrates from C1 and C4 Feedstocks. *Nat. Chem.* **2023**, 856–861. https://doi.org/10.1038/s41557-023-01187-0.
(35) Dong, X.; Robinson, J. R. The Role of Neutral Donor Ligands in the Isoselective Ring-Opening Polymerization of Rac-β-Butyrolactone. *Chem. Sci.* **2020**, *11* (31), 8184–8195. https://doi.org/10.1039/D0SC03507F.
(36) Bruckmoser, J.; Pongratz, S.; Stieglitz, L.; Rieger, B. Highly Isoselective Ring-Opening Polymerization of Rac-β-Butyrolactone: Access to Synthetic Poly(3-Hydroxybutyrate) with Polyolefin-like Material Properties. *J. Am. Chem. Soc.* **2023**, *145* (21), 11494–11498. https://doi.org/10.1021/jacs.3c02348.
(37) Zhuo, Z.; Zhang, C.; Luo, Y.; Wang, Y.; Yao, Y.; Yuan, D.; Cui, D. Stereo-Selectivity Switchable ROP of Rac-β-Butyrolactone Initiated by Salan-Ligated Rare-Earth Metal Amide Complexes: The Key Role of the Substituents on Ligand Frameworks. *Chem. Commun.* **2018**, *54* (85), 11998–12001. https://doi.org/10.1039/C8CC05469J.
(38) Kramer, J. W.; Treitler, D. S.; Dunn, E. W.; Castro, P. M.; Roisnel, T.; Thomas, C. M.; Coates, G. W. Polymerization of Enantiopure Monomers Using Syndiospecific Catalysts: A New Approach To Sequence Control in Polymer Synthesis. *J. Am. Chem. Soc.* **2009**, *131* (44), 16042–16044. https://doi.org/10.1021/ja9075327.

(39) Li, H.; Ollivier, J.; Guillaume, S. M.; Carpentier, J.-F. Tacticity Control of Cyclic Poly(3-Thiobutyrate) Prepared by Ring-Opening Polymerization of Racemic β-Thiobutyrolactone. *Angew. Chem. Int. Ed.* **2022**, *61* (21), e202202386. https://doi.org/https://doi.org/10.1002/anie.202202386.

(40) Kim, D. H.; Kim, Y. J. Synthesis and Inhibitory Activity of Optically Active 2-Benzyl-3-Mercaptopropanoic Acid against Carboxypeptidase A. *Bioorg. Med. Chem. Lett.* **1993**, *3* (12), 2681–2684. https://doi.org/https://doi.org/10.1016/S0960-894X(01)80741-1.

(41) Noble, F.; Smadja, C.; Valverde, O.; Maldonado, R.; Coric, P.; Turcaud, S.; Fournié-Zaluski, M.-C.; Roques, B. P. Pain-Suppressive Effects on Various Nociceptive Stimuli (Thermal, Chemical, Electrical and Inflammatory) of the First Orally Active Enkephalin-Metabolizing Enzyme Inhibitor RB 120. *Pain* **1997**, *73* (3).

(42) Crich, D.; Sana, K. SN2-Type Nucleophilic Opening of β-Thiolactones (Thietan-2-Ones) as a Source of Thioacids for Coupling Reactions. *J. Org. Chem.* **2009**, *74* (9), 3389–3393. https://doi.org/10.1021/jo9001728.

(43) Li, H.; Shakaroun, R. M.; Guillaume, S. M.; Carpentier, J. F. Recent Advances in Metal-Mediated Stereoselective Ring-Opening Polymerization of Functional Cyclic Esters towards Well-Defined Poly(Hydroxy Acid)s: From Stereoselectivity to Sequence-Control. *Chem. Eur. J.* **2020**, *26* (1), 128–138. https://doi.org/10.1002/chem.201904108.

(44) Cheng, M.; Attygalle, A. B.; Lobkovsky, E. B.; Coates, G. W. Single-Site Catalysts for Ring-Opening Polymerization: Synthesis of Heterotactic Poly(Lactic Acid) from Rac-Lactide. *J. Am. Chem. Soc.* **1999**, *121* (49), 11583–11584. https://doi.org/10.1021/ja992678o.

(45) MacDonald, J. P.; Shaver, M. P. Aluminum Salen and Salan Polymerization Catalysts: From Monomer Scope to Macrostructure Control. In *Green Polymer Chemistry: Biobased Materials and Biocatalysis*; ACS Symposium Series; American Chemical Society, 2015; Vol. 1192, pp 10–147. https://doi.org/doi:10.1021/bk-2015-1192.ch010.

(46) Spassky, N.; Wisniewski, M.; Pluta, C.; Le Borgne, A. Highly Stereoelective Polymerization of Rac-(D,L)-Lactide with a Chiral Schiff's Base/Aluminium Alkoxide Initiator. *Macromol. Chem. Phys.* **1996**, *197* (9), 2627–2637. https://doi.org/https://doi.org/10.1002/macp.1996.021970902.

(47) Ovitt, T. M.; Coates, G. W. Stereoselective Ring-Opening Polymerization of Meso-Lactide: Synthesis of Syndiotactic Poly(Lactic Acid). *J. Am. Chem. Soc.* **1999**, *121* (16), 4072–4073. https://doi.org/10.1021/ja990088k.

(48) Lu, Y.; Coates, G. W. Pairing-Enhanced Regioselectivity: Synthesis of Alternating Poly(Lactic-Co-Glycolic Acid) from Racemic Methyl-Glycolide. *J. Am. Chem. Soc.* **2023**, *145* (41), 22425–22432. https://doi.org/10.1021/jacs.3c05941.

(49) Grassie, N.; Murray, E. J.; Holmes, P. A. The Thermal Degradation of Poly(-(d)-β-Hydroxybutyric Acid): Part 3—The Reaction Mechanism. *Polym. Degrad. Stab.* **1984**, *6* (3), 127–134. https://doi.org/https://doi.org/10.1016/0141-3910(84)90032-6.

(50) Larsson, M.; Markbo, O.; Jannasch, P. Melt Processability and Thermomechanical Properties of Blends Based on Polyhydroxyalkanoates and Poly(Butylene Adipate-Co-Terephthalate). *RSC Adv.* **2016**, *6* (50), 44354–44363. https://doi.org/10.1039/C6RA06282B.

(51) Poras, H.; Bonnard, E.; Dangé, E.; Fournié-Zaluski, M.-C.; Roques, B. P. New Orally Active Dual Enkephalinase Inhibitors (DENKIs) for Central and Peripheral Pain Treatment. *J. Med. Chem.* **2014**, *57* (13), 5748–5763. https://doi.org/10.1021/jm500602h.

(52) Poras, H.; Lefebvre, L.; Zhao, X.; Gamberoni, L.; De Rosa, S.; Velardi, R. Industrial Process for the Preparation of (5S,10S)-10-Benzyl-16-Methyl-11,14,18-Trioxo-15,17,19-Trioxa-2,7,8-Trithia-12-Azahenicosan-5-Aminium (E)-3-Carboxyacrylate Salt. WO 2017/064250A1 2017-04-20.

(53) Lipinski, B. M.; Morris, L. S.; Silberstein, M. N.; Coates, G. W. Isotactic Poly(Propylene Oxide): A Photodegradable Polymer with Strain Hardening Properties. *J. Am. Chem. Soc.* **2020**, *142* (14), 6800–6806. https://doi.org/10.1021/jacs.0c01768.